

20 CM VLA RADIO-CONTINUUM STUDY OF M 31 – IMAGES AND POINT SOURCE CATALOGUES

T. J. Galvin, M. D. Filipović, E. J. Crawford, N. F. H. Tothill, G. F. Wong, A. Y. De Horta

University of Western Sydney, Locked Bag 1797, Penrith South DC, NSW 2751, AUSTRALIA
E-mail: *m.filipovic@uws.edu.au*

(Received: April 23, 2012; Accepted: April 27, 2012)

SUMMARY: We present a series of new high-sensitivity and high-resolution radio-continuum images of M 31 at $\lambda=20$ cm ($\nu=1.4$ GHz). These new images were produced by merging archived 20 cm radio-continuum observations from the Very Large Array (VLA) telescope. Images presented here are sensitive to $\text{rms}=60 \mu\text{Jy}$ and feature high angular resolution ($<10''$). A complete sample of discrete radio sources have been catalogued and analysed across 17 individual VLA projects. We identified a total of 864 unique discrete radio sources across the field of M 31. One of the most prominent regions in M 31 is the ring feature for which we estimated total integrated flux of 706 mJy at $\lambda=20$ cm. We compare here, detected sources to those listed in Gelfand et al. (2004) at $\lambda=92$ cm and find 118 sources in common to both surveys. The majority (61%) of these sources exhibit a spectral index of $\alpha < -0.6$ indicating that their emission is predominantly non-thermal in nature. That is more typical for background objects.

Key words. Techniques: image processing – Radio Continuum – Catalogs

1. INTRODUCTION

A member of the Andromeda constellation M 31 at a distance of ~ 778 Kpc (Karachentsev et al. 2004), is the closest spiral galaxy to our own. For this reason, it plays a significant role in galactic and extragalactic studies. A number of previous radio-continuum studies at $\lambda=20$ cm (Braun 1990a) focused on general properties of M 31, such as its structure and magnetic fields. Also, Braun (1990b) presented a list of 20-cm sources (534) in the north-east parts of M 31. A number of other studies such as Dickel et al. (1982) estimated flux densities of M 31 supernova remnants (SNRs) and H II regions.

In this paper, we reexamine all available archived radio-continuum observations performed with the Very Large Array (VLA) at $\lambda=20$ cm

($\nu=1.4$ GHz) with the intention of merging these observations into a single mosaic radio-continuum image. By combining a large amount of existing data, while using the latest generation of computing power, we can create new images that feature both high angular resolution and improved sensitivity. The newly constructed images are analysed and the difference between the various M 31 images created at 20 cm are discussed.

In §2 we describe the observational data and reduction techniques. In §3 we present our new maps and a brief discussion. Source catalogues are given in §4 and §5 is the conclusion.

2. DATA

A collection of existing, archived radio-continuum observations at $\lambda=20$ cm with pointings centred on M31 were obtained from the National Radio Astronomy Observatory (NRAO)¹ online data retrieval system. In total, 15 VLA projects with a variety of array configurations were selected for use in this study, as summarised in Table 1. These projects were observed between the 1st of October 1983 and 27th of September 1997 and are comprised of 28 individual observational runs.

3. Image Creation

The MIRIAD (Sault et al. 1995) and KARMA (Gooch 1996) software packages were used for data reduction and analysis. Because of the large volume of data, the MIRIAD package was compiled to run on a 16-processor high-performance computer system.

Initially, observations were imported into AIPS using the task FILLM, and then all sources were split with SPLIT. Using the task UVFIX, source coordinates were converted from the B1950 to the J2000 reference frame and the task FITTP was used to export each source to a FITS file.

The MIRIAD package was then used for actual data reduction. The task ATLOD was used to convert ATCA observations into MIRIAD files, while the task FITS was used to import the previous AIPS-produced fits files and convert them to MIRIAD files. Typical calibration and flagging procedures were then carried out (Sault et al. 1995). Using the task INVERT, each project was imaged individually using a natural weighting scheme. Images with a single pointing were cleaned using the task CLEAN, while each mo-

saic image was cleaned using the task MOSSDI. Each of these cleaning tasks uses a SDI clean algorithm to reduce image artefacts (Steer et al. 1984). To convolve a clean model the task RESTOR was then used on each of the cleaned maps, followed by LINMOS to correct for the primary beam for single pointing observations. For more information on data analysis and image creation see Galvin et al. (2012) and Payne et al. (2004).

The catalogue of radio-continuum sources contains positions RA(J2000), Dec(J2000) and integrated flux densities at 13 cm (Table A1), 20 cm (Table A2) and 36 cm (Table A3). Table 3 contains the r.m.s., number of sources detected, number of sources identified within the field of the 13 cm image and beam size for each image.

4. RESULTS

By comparing the individual maps produced from a variety of observations, the effects of varying array configurations can be seen, as shown in Figs. 1–18. For example, projects AC0101 and AB0551 show a region of extended emission with poorly resolved point sources across all individual images. This can be attributed to the short baselines of the D type configuration used by the VLA to produce each of these images.

As expected, observations conducted with a C and B type array configuration, such as AM0464 and AT0149 respectively, demonstrate a progressive loss of extended emission and improved point source resolution across their field of view. Observations that used an A type configuration, such as AH0139 and AH0221, show a significant loss of extended emission but better point source resolution.

¹<https://archive.nrao.edu/archive/e2earchivex.jsp>

Table 1.List of VLA projects of M31 used in this study. RA and DEC represent coordinates of central pointings.

<i>Project ID</i>	<i>RA</i> h m s	<i>DEC</i> ° ' "	<i>Array Config</i>	<i>Date</i>	<i>Freq.</i> (MHz)	<i>Bandwidth</i> (MHz)	<i>Time on Source</i> (hrs)	<i>Recorded Polarisation</i>	<i>Primary Calibrator</i>	<i>Secondary Calibrator</i>
AH0139	00:42:44.24	41:16:25.65	A	01/10/1983	1465, 1515	50	1.18	rr, ll, rl, lr	1328+307	0107+562
AH0221	00:43:20.37	41:13:00.17	A	06/04/1986	1465	50	0.61	rr, ll, rl, lr	0137+331	0026+346
AH0221	00:43:44.50	41:17:34.87	A	06/04/1986	1465	50	0.61	rr, ll, rl, lr	0137+331	0026+346
AH0221	00:40:13.76	40:50:06.55	A	06/04/1986	1465	50	0.64	rr, ll, rl, lr	0137+331	0026+346
AH0221	00:45:36.88	41:03:53.32	A	06/04/1986	1465	50	0.62	rr, ll, rl, lr	0137+331	0026+346
AH0221	00:46:00.39	42:06:22.99	A	06/04/1986	1465	50	0.56	rr, ll, rl, lr	0137+331	0026+346
AH0221	00:46:56.73	42:20:27.18	A	06/04/1986	1465	50	0.64	rr, ll, rl, lr	0137+331	0026+346
AH0221	00:48:03.74	41:40:53.21	A	06/04/1986	1465	50	0.65	rr, ll, rl, lr	0137+331	0026+346
AH0221	00:41:30.83	40:58:32.59	A	06/04/1986	1465	50	0.49	rr, ll, rl, lr	0137+331	0026+346
AH0221	00:42:03.74	40:20:31.17	A	06/04/1986	1465	50	0.61	rr, ll, rl, lr	0137+331	0026+346
AH0221	00:42:20.03	40:57:40.96	A	06/04/1986	1465	50	0.63	rr, ll, rl, lr	0137+331	0026+346
AH0221	00:42:30.20	41:19:25.83	A	06/04/1986	1465	50	0.63	rr, ll, rl, lr	0137+331	0026+346
AH0221	00:42:30.14	41:09:25.84	A	06/04/1986	1465	50	0.63	rr, ll, rl, lr	0137+331	0026+346
AH0221	00:42:56.31	41:19:25.49	A	06/04/1986	1465	50	0.61	rr, ll, rl, lr	0137+331	0026+346
AH0221	00:42:56.25	41:09:25.50	A	06/04/1986	1465	50	0.61	rr, ll, rl, lr	0137+331	0026+346
AH0221	00:43:09.17	40:48:03.41	A	06/04/1986	1465	50	0.63	rr, ll, rl, lr	0137+331	0026+346
AT0149	00:42:41.02	41:15:30.69	B	18/04/1993	1385, 1465	50	0.06	rr, ll, rl, lr	0137+331	0248+430
AB0679	00:42:46.05	41:16:11.63	C	26/08/1993	1365, 1465	50	6.55	rr, ll, rl, lr	0137+331	0038+328
AB0679	00:42:46:05	41:16:11.63	C	29/08/1993	1365, 1465	50	14.02	rr, ll, rl, lr	0137+331	0038+328
AH0524	00:41:25.89	41:12:26.66	C	18/12/1994	1365, 1465	50	4.74	rr, ll, rl, lr	0137+331	0026+346
AM0464	00:40:20.00	40:31:30.00	C	01/11/1994	1385, 1415	50	1.07	rr, ll, rl, lr	0137+331	0029+349
AM0464	00:41:05.00	40:46:30.00	C	01/11/1994	1385, 1415	50	1.05	rr, ll, rl, lr	0137+331	0029+349
AM0464	00:41:05.00	41:04:45.00	C	01/11/1994	1385, 1415	50	1.05	rr, ll, rl, lr	0137+331	0029+349
AM0464	00:42:45.00	41:04:25.00	C	01/11/1994	1385, 1415	50	1.06	rr, ll, rl, lr	0137+331	0029+349
AM0464	00:44:00.00	41:34:25.00	C	01/11/1994	1385, 1415	50	1.06	rr, ll, rl, lr	0137+331	0029+349
AM0464	00:44:30.00	41:22:25.00	C	01/11/1994	1385, 1415	50	1.05	rr, ll, rl, lr	0137+331	0029+349
AM0464	00:45:40.00	41:47:09.00	C	01/11/1994	1385, 1415	50	1.06	rr, ll, rl, lr	0137+331	0029+349
AC0496	00:42:35.44	41:57:46.80	C	27/09/1997	1365, 1435	50	0.04	rr, ll, rl, lr	0137+331	0102+584
AC0101	00:42:44.54	41:16:28.65	D	13/07/1984	1465, 1515	50	0.10	rr, ll, rl, lr	0137+331	2234+282
AB0551	00:42:46.05	41:16:11.63	D	27/07/1989	1465, 1515	50	4.38	rr, ll, rl, lr	0038+328	
AB0491	00:42:05.93	40:50:26.15	D	08/09/1988	1465	50	8.66	rr, ll, rl, lr	1328+307	0026+346
AB0647	00:44:49.83	41:26:23.97	D	(25,27)/07/1992	1465, 1515	50	3.01, 2.60	rr, ll, rl, lr	0137+331	0038+328
AB0647	00:45:08.07	41:51:23.72	D	(25,27)/07/1992	1465, 1515	50	2.99, 2.57	rr, ll, rl, lr	0137+331	0038+328
AB0437	00:43:43.64	40:58:27.19	D	04/04/1987	1465, 1515	50	8.86	rr, ll, rl, lr	0137+331	0038+328
AB0437	00:40:13.44	40:46:27.56	D	13/04/1987	1465, 1515	50	8.84	rr, ll, rl, lr	0137+331	0038+328
AC0308	00:42:00.00	40:41:42.00	D	08/09/1996	1365, 1435	50	0.01	rr, ll, rl, lr	0521+166	0141+138
AC0308	00:42:00.00	41:13:12.00	D	08/09/1996	1365, 1435	50	0.01	rr, ll, rl, lr	0521+166	0141+138

4	AC0308	00:43:30.00	40:57:30.00	D	08/09/1996	1365, 1435	50	0.01	rr,ll,rl,lr	0521+166	0141+138
	AC0308	00:43:30.00	41:29:06.00	D	08/09/1996	1365, 1435	50	0.01	rr,ll,rl,lr	0521+166	0141+138
	AC0308	00:43:30.00	42:01:00.00	D	08/09/1996	1365, 1435	50	0.01	rr,ll,rl,lr	0521+166	0141+138
	AC0308	00:45:00.00	41:13:12.00	D	20/09/1996	1365, 1435	50	0.01	rr,ll,rl,lr	0521+166	2202+422
	AC0308	00:45:00.00	42:17:00.00	D	20/09/1996	1365, 1435	50	0.01	rr,ll,rl,lr	0521+166	2202+422
	AC0308	00:46:30.00	41:29:06.00	D	20/09/1996	1365, 1435	50	0.01	rr,ll,rl,lr	0521+166	2202+422
	AC0308	00:46:30.00	42:01:00.00	D	20/09/1996	1365, 1435	50	0.01	rr,ll,rl,lr	0521+166	2202+422
	AC0308	00:39:00.00	40:10:24.00	D	24/09/1996	1365, 1435	50	0.01	rr,ll,rl,lr	0521+166	2202+422
	AC0308	00:39:00.00	40:41:42.00	D	24/09/1996	1365, 1435	50	0.01	rr,ll,rl,lr	0521+166	2202+422
	AC0308	00:40:30.00	40:26:06.00	D	24/09/1996	1365, 1435	50	0.01	rr,ll,rl,lr	0521+166	2202+422
	AC0308	00:40:30.00	40:57:30.00	D	24/09/1996	1365, 1435	50	0.01	rr,ll,rl,lr	0521+166	2202+422
	AC0308	00:40:30.00	41:29:06.00	D	24/09/1996	1365, 1435	50	0.01	rr,ll,rl,lr	0521+166	2202+422
	AB0396	00:42:46.05	41:16:11.62	B	27/07/1986	1465	50	0.97	RCP	1328+307	2352+495
	AB0396	00:42:46.05	41:16:11.62	B	(18,29)/08/1986	1465	50	0.94, 0.92	RCP	1328+307	2352+495
	AB0396	00:42:46.05	41:16:11.62	B	04/09/1986	1465	50	1.64	RCP	1328+307	2352+495
	AB0396	00:43:58.16	41:33:32.67	B	27/07/1986	1465	50	0.97	RCP	1328+307	2352+495
	AB0396	00:43:58.16	41:33:32.67	B	(18,29)/08/1986	1465	50	0.94, 0.92	RCP	1328+307	2352+495
	AB0396	00:43:58.16	41:33:32.67	B	04/09/1986	1465	50	0.92	RCP	1328+307	2352+495
	AB0396	00:45:10.98	41:50:50.67	B	27/07/1986	1465	50	0.96	RCP	1328+307	2352+495
	AB0396	00:45:10.98	41:50:50.67	B	(18,29)/08/1986	1465	50	0.93, 0.93	RCP	1328+307	2352+495
	AB0396	00:45:10.98	41:50:50.67	B	04/09/1986	1465	50	0.93	RCP	1328+307	2352+495
	AB0396	00:46:24.41	42:08:05.64	B	27/07/1986	1465	50	0.80	RCP	1328+307	2352+495
	AB0396	00:46:24.41	42:08:05.64	B	(18,29)/08/1986	1465	50	0.93, 0.92	RCP	1328+307	2352+495
	AB0396	00:46:24.41	42:08:05.64	B	04/09/1986	1465	50	0.92	RCP	1328+307	2352+495
	AB0396	00:44:08.20	41:18:06.53	B	27/07/1986	1465	50	0.96	RCP	1328+307	2352+495
	AB0396	00:44:08.20	41:18:06.53	B	(18,29)/08/1986	1465	50	0.92, 0.93	RCP	1328+307	2352+495
	AB0396	00:44:08.20	41:18:06.53	B	04/09/1986	1465	50	0.91	RCP	1328+307	2352+495
	AB0396	00:45:20.82	41:35:23.54	B	27/07/1986	1465	50	0.95	RCP	1328+307	2352+495
	AB0396	00:45:20.82	41:35:23.54	B	(18,29)/08/1986	1465	50	0.92, 0.92	RCP	1328+307	2352+495
	AB0396	00:45:20.82	41:35:23.54	B	04/09/1986	1465	50	0.93	RCP	1328+307	2352+495
	AB0396	00:46:33.94	41:52:38.51	B	27/07/1986	1465	50	0.96	RCP	1328+307	2352+495
	AB0396	00:46:33.94	41:52:38.51	B	(18,29)/08/1986	1465	50	0.93, 0.92	RCP	1328+307	2352+495
	AB0396	00:46:33.94	41:52:38.51	B	04/09/1986	1465	50	0.93	RCP	1328+307	2352+495
	AB0396	00:42:35.70	41:31:37.76	B	27/07/1986	1465	50	0.96	RCP	1328+307	2352+495
	AB0396	00:42:35.70	41:31:37.76	B	(18,29)/08/1986	1465	50	0.92, 0.92	RCP	1328+307	2352+495
	AB0396	00:42:35.70	41:31:37.76	B	04/09/1986	1465	50	0.93	RCP	1328+307	2352+495
	AB0396	00:43:48.11	41:48:58.80	B	27/07/1986	1465	50	0.96	RCP	1328+307	2352+495
	AB0396	00:43:48.11	41:48:58.80	B	(18,29)/08/1986	1465	50	0.92, 0.92	RCP	1328+307	2352+495
	AB0396	00:43:48.11	41:48:58.80	B	04/09/1986	1465	50	0.93	RCP	1328+307	2352+495
	AB0396	00:45:01.14	42:06:17.81	B	27/07/1986	1465	50	0.96	RCP	1328+307	2352+495
	AB0396	00:45:01.14	42:06:17.81	B	(18,29)/08/1986	1465	50	0.93, 0.93	RCP	1328+307	2352+495

AB0396	00:45:01.14	42:06:17.81	B	04/09/1986	1465	50	0.93	RCP	1328+307	2352+495
AB0396	00:42:46.05	41:16:11.62	C	14/12/1986	1465	50	0.93	RCP	1328+307	2352+495
AB0396	00:43:58.16	41:33:32.67	C	14/12/1986	1465	50	0.93	RCP	1328+307	2352+495
AB0396	00:45:10.98	41:50:50.67	C	14/12/1986	1465	50	0.92	RCP	1328+307	2352+495
AB0396	00:46:24.41	42:08:05.64	C	14/12/1986	1465	50	0.92	RCP	1328+307	2352+495
AB0396	00:44:08.20	41:18:06.53	C	14/12/1986	1465	50	0.93	RCP	1328+307	2352+495
AB0396	00:45:20.82	41:35:23.54	C	14/12/1986	1465	50	0.94	RCP	1328+307	2352+495
AB0396	00:46:33.94	41:52:38.51	C	14/12/1986	1465	50	0.93	RCP	1328+307	2352+495
AB0396	00:42:35.70	41:31:37.76	C	14/12/1986	1465	50	0.93	RCP	1328+307	2352+495
AB0396	00:43:48.11	41:48:58.80	C	14/12/1986	1465	50	0.93	RCP	1328+307	2352+495
AB0396	00:45:01.14	42:06:17.81	C	14/12/1986	1465	50	0.89	RCP	1328+307	2352+495
AB0396	00:45:10.98	41:50:50.67	D	13/03/1986	1465	50	0.90	RCP	1328+307	2352+495
AB0396	00:46:24.41	42:08:05.64	D	13/03/1986	1465	50	0.85	RCP	1328+307	2352+495
AB0396	00:45:20.82	41:35:23.54	D	13/03/1986	1465	50	0.74	RCP	1328+307	2352+495
AB0396	00:46:33.94	41:52:38.51	D	13/03/1986	1465	50	0.80	RCP	1328+307	2352+495
AB0396	00:43:48.11	41:48:58.80	D	13/03/1986	1465	50	0.89	RCP	1328+307	2352+495
AB0396	00:45:01.14	42:06:17.81	D	13/03/1986	1465	50	0.88	RCP	0137+331	0137+331
AB0999	00:42:46.05	41:16:11.62	D	23/01/1986	1465	50	0.20	RCP	0137+331	0137+331
AB0999	00:43:58.16	41:33:32.67	D	23/01/1986	1465	50	0.26	RCP	0137+331	0137+331
AB0999	00:45:10.98	41:50:50.67	D	23/01/1986	1465	50	0.20	RCP	0137+331	0137+331
AB0999	00:46:24.41	42:08:05.64	D	23/01/1986	1465	50	0.17	RCP	0137+331	0137+331
AB0999	00:44:08.20	41:18:06.53	D	23/01/1986	1465	50	0.27	RCP	0137+331	0137+331
AB0999	00:45:20.82	41:35:23.54	D	23/01/1986	1465	50	0.27	RCP	0137+331	0137+331
AB0999	00:46:33.94	41:52:38.51	D	23/01/1986	1465	50	0.25	RCP	0137+331	0137+331
AB0999	00:42:35.70	41:31:37.76	D	23/01/1986	1465	50	0.27	RCP	0137+331	0137+331
AB0999	00:43:48.11	41:48:58.80	D	23/01/1986	1465	50	0.27	RCP	0137+331	0137+331
AB0999	00:45:01.14	42:06:17.81	D	23/01/1986	1465	50	0.27	RCP	0137+331	0137+331

Table 2.The details of VLA single and merged projects of M 31 mosaics at 20 cm.

VLA Project	Beam Size (arcsec)	r.m.s. (mJy/beam)	Figure
AC0101-a	45.9×43.2	0.49	1
AB0551-a	35.9×32.1	0.12	2
AB0491-a	39.0×33.8	0.12	3
AB0647-a	41.2×37.3	0.24	4
AB0647-b	40.9×35.4	0.24	5
AB0437-a	36.0×31.0	0.10	6
AB0437-b	36.0×31.1	0.19	7
AC0308-a	57.9×49.8	0.72	8
AC0308-b	58.9×48.9	0.54	9
AC0308-c	58.0×50.2	0.60	10
AC0496-a	54.6×14.0	0.08	11
AM0464-a	12.8×12.2	0.13	12
AH0524-a	12.8×12.2	0.07	13
AB0679-a	12.0×11.7	0.07	14
AB0679-b	12.1×11.5	0.08	15
AT0149-a	4.0×3.4	0.08	16
AH0221-a	3.4×3.2	0.22	17
AH0139-a	7.2×6.6	0.16	18
Fully Polarised (5 k λ restricted)	35.73×16.38	0.15	19
Fully Polarised (25 k λ restricted)	6.4×5.4	0.09	20
Mosaic AB0396 and AB0999 (35 k λ restricted)	4.6×3.8	0.08	21
All Calibrated (5 k λ restricted)	32.6×16.4	0.13	22
All Calibrated (25 k λ restricted)	6.1×5.4	0.12	23

4.1 New Combined M 31 Mosaics at $\lambda=20$ cm

Figs. 19 and 20 are the resulting images when all fully polarised VLA observations are merged together. Both images suffer from artefacts around the outer region of the field of view. This can be attributed to the image stacking process, where observations conducted with the use of a compact array configuration get stretched to meet the resolution of the image as a whole.

Fig. 19 shows the resulting radio-continuum image when all fully polarised VLA observations are merged together with a restricted uv coverage of 0-5 k λ . This restriction was introduced in order to preserve the intricate structure of the extended emission while partly resolving point sources across the field.

Fig. 20 is the same data-set as Fig.19 with a restricted uv coverage of 0-25 k λ . This restriction was imposed after a trial and error process where we identified the MIRIAD's software limitations. Despite this restriction, point sources are well resolved and there remains a region of extended emission.

Fig. 21 shows a mosaic radio-continuum image of VLA projects AB0396 and AB0999 with a restricted uv coverage of 0-35 k λ . Point sources are seen prominently across the field of view with little extended emission. This can be attributed to

the larger array configurations, and thus longer baselines, which these observations are constructed of.

Fig. 22 is a mosaic radio-continuum image comprised of all calibrated VLA observations from this study with a restricted uv coverage of 0-5 k λ . This restriction was implemented to place greater emphasis on the intrinsic structure of the extended emission throughout the field of view. The majority of observations within VLA projects AB0396 and AB0999 were made with B configuration types. This provided uv coverage data that was noticeably absent in other observations. This has significantly improved the overall clarity of the image when compared to Fig. 19. One of the most prominent regions in M 31 is the ring feature for which we estimated total integrated flux of 706 ± 35 mJy.

In Fig. 23, we show the resulting image when all calibrated VLA observations are merged together with a restricted uv coverage of 0-25 k λ . Again, this restricted uv coverage was used to overcome the limit of the MIRIAD software imaging capabilities. Point sources are well resolved and there remains a region of extended emission.

5. DISCRETE RADIO-CONTINUUM SOURCES IN THE FIELD OF M 31

For each project imaged, a source catalogue was created. Tables 3, 4, 5, 6, 7, 8, 9, 10, 11, 12, 13, 14, 15, 16, 17, 18, 19 and 20 list sources found in each individual project that has been imaged in this study. These catalogues contain a source's RA and DEC positions (J2000) and integrated flux density. All catalogues have been cross referenced and sources common to multiple projects have been noted in Col. 6 of each table.

Across fifteen individual and three merged projects, a total of 864 unique discrete sources are identified. We compared these discrete sources to those listed in Gelfand et al. (2004) at $\lambda=92$ cm and found 118 sources in common to both surveys. Table 21 is an extract of this comparison, where Col. 11 is the estimated spectral index ($S_\nu \propto \nu^\alpha$) of each source. The complete list and all catalogues can be found in on-line archive (<http://cds.u-strasbg.fr/>).

The average flux density, as listed in Col. 5 of Table 21, was calculated by averaging flux den-

sity from each project where a discrete source was found. A sources error, as listed in Col. 6, was calculated by finding the largest difference between the average flux density of a source, and the flux density from each project it appeared in. In the case where a source was found in multiple projects, its name, project, RA and DEC, as listed in Cols. 1, 2, 3 and 4, were taken from the highest resolution image.

In Fig 24 we compare the RA and DEC between our 20 cm catalogue and Gelfand et al. (2004) sources as listed in Table 21. The concentration of points near the centre of graph indicates an accurate model for comparison. We found that the average positional difference in ΔRA and ΔDEC is $-0.01''$ (with a SD of $1.912''$) and $+0.18''$ (with a SD of $1.543''$) respectively.

Fig 25 shows the spectral index distribution of sources listed in Table 21. The majority (61%) of sources exhibit a spectral index of <-0.6 indicating that their emission is predominantly non-thermal in nature. This implies that most of these sources will be background ANGs or Quasars. Some of these background source could qualify as compact steep spectrum sources.

Table 3. Sample list of sources at 20 cm found in Project AB0437-a

1 #	2 Name	3 RA (J2000)	4 DEC (J2000)	5 Flux (mJy)	6 Notes
1	J003904+410822	00:39:04.30	+41:08:22.20	2.46	
2	J003907+410346	00:39:07.94	+41:03:46.10	20.65	
3	J003908+410338	00:39:08.28	+41:03:38.21	7.59	
4	J003918+410301	00:39:18.15	+41:03:01.10	12.43	
5	J003918+411634	00:39:18.88	+41:16:34.06	5.65	

Table 4. Sample list of sources at 20 cm found in Project AB0437-b.

1 #	2 Name	3 RA (J2000)	4 DEC (J2000)	5 Flux (mJy)	6 Notes
1	J003839+403300	00:38:39.00	+40:33:00.60	4.85	
2	J003908+403007	00:39:08.25	+40:30:07.71	2.88	
3	J003908+410335	00:39:08.39	+41:03:35.80	6.62	
4	J003917+410258	00:39:17.98	+41:02:58.90	9.85	
5	J003927+405425	00:39:27.05	+40:54:25.00	4.61	

Table 5. Sample list of sources at 20 cm found in Project AB0491-a. Column 6 describes the source in additional projects.

1 #	2 Name	3 RA (J2000)	4 DEC (J2000)	5 Flux (mJy)	6 Notes
1	J004013+405005	00:40:13.84	+40:50:05.9	41.99	Table:17 #6
2	J004017+405824	00:40:17.03	+40:58:24.8	21.55	Table:17 #8
3	J004024+410711	00:40:24.78	+41:07:11.3	26.70	Table:19 #24
4	J004036+411910	00:40:36.91	+41:19:10.9	15270.00	
5	J004044+404845	00:40:44.56	+40:48:45.3	13.30	

Table 6. Sample list of sources at 20 cm found in Project AB0551-a. Column 6 describes the source in additional projects.

1 #	2 Name	3 RA (J2000)	4 DEC (J2000)	5 Flux (mJy)	6 Notes
1	J004056+405734	00:40:56.81	+40:57:34.31	13.90	
2	J004100+411358	00:41:00.71	+41:13:58.30	5.53	
3	J004109+412456	00:41:09.61	+41:24:56.80	27.57	
4	J004117+412316	00:41:17.91	+41:23:16.22	2.16	
5	J004120+411044	00:41:20.12	+41:10:44.7	18.97	Table:9 #3, Table:10 #5

Table 7. Sample list of sources at 20 cm found in Project AB0647-a.

1 #	2 Name	3 RA (J2000)	4 DEC (J2000)	5 Flux (mJy)	6 Notes
1	J004132+412429	00:41:32.19	+41:24:29.20	2.13	
2	J004139+414252	00:41:39.59	+41:42:52.90	2.87	
3	J004139+413040	00:41:39.64	+41:30:40.80	5.69	
4	J004155+413720	00:41:55.95	+41:37:20.10	1.93	
5	J004212+414828	00:42:12.82	+41:48:28.00	4.40	

Table 8. Sample list of sources at 20 cm found in Project AB0647-b. Column 6 describes the source in additional projects..

1 #	2 Name	3 RA (J2000)	4 DEC (J2000)	5 Flux (mJy)	6 Notes
1	J004200+415408	00:42:00.51	+41:54:08.4	0.76	
2	J004204+412932	00:42:04.53	+41:29:32.3	2.41	
3	J004218+412930	00:42:18.89	+41:29:30.6	155.90	Table:7 #6
4	J004233+412929	00:42:33.41	+41:29:29.7	2.92	
5	J004235+415743	00:42:35.77	+41:57:43.4	24.40	Table:7 #7

Table 9. Sample list of sources at 20 cm found in Project AB0679-a. Column 6 describes the source in additional projects.

1 #	2 Name	3 RA (J2000)	4 DEC (J2000)	5 Flux (mJy)	6 Notes
1	J004108+412454	00:41:08.11	+41:24:54.7	10.76	Table:10 #1
2	J004112+412458	00:41:12.10	+41:24:58.6	44.01	
3	J004120+411045	00:41:20.18	+41:10:45.3	19.68	Table:6 #5, Table:10 #5
4	J004139+413031	00:41:39.60	+41:30:31.3	32.32	Table:12 #20, Table:6 #7, Table:10 #6
5	J004141+410338	00:41:41.50	+41:03:38.9	45.71	Table:6 #8, Table:10 #8

Table 10. Sample list of sources at 20 cm found in Project AB0679-b. Column 6 describes the source in additional projects.

1 #	2 Name	3 RA (J2000)	4 DEC (J2000)	5 Flux (mJy)	6 Notes
1	J004108+412455	00:41:08.18	+41:24:55.20	13.54	
2	J004112+412458	00:41:12.32	+41:24:58.10	4.45	
3	J004114+412454	00:41:14.03	+41:24:54.40	3.03	
4	J004119+412314	00:41:19.17	+41:23:14.37	1.09	
5	J004120+411045	00:41:20.17	+41:10:45.1	19.05	Table:6 #5

Table 11. Sample list of sources at 20 cm found in Project AC0101-a.

1 #	2 Name	3 RA (J2000)	4 DEC (J2000)	5 Flux (mJy)	6 Notes
1	J004057+412133	00:40:57.97	+41:21:33.30	10.70	
2	J004107+412129	00:41:07.74	+41:21:29.70	6.36	
3	J004108+412444	00:41:08.09	+41:24:44.50	13.49	
4	J004120+411042	00:41:20.00	+41:10:42.30	15.50	
5	J004139+413035	00:41:39.65	+41:30:35.70	27.95	

Table 12. Sample list of sources at 20 cm found in Project AC0308-a.

1 #	2 Name	3 RA (J2000)	4 DEC (J2000)	5 Flux (mJy)	6 Notes
1	J003938+410327	00:39:38.55	+41:03:27.90	5.31	
2	J003957+411138	00:39:57.13	+41:11:38.70	11.93	
3	J004002+412634	00:40:02.34	+41:26:34.40	5.37	
4	J004010+411825	00:40:10.88	+41:18:25.90	3.47	
5	J004014+410841	00:40:14.02	+41:08:41.10	14.23	

Table 13. Sample list of sources at 20 cm found in Project AC0308-b.

1 #	2 Name	3 RA (J2000)	4 DEC (J2000)	5 Flux (mJy)	6 Notes
1	J004257+411643	00:42:57.84	+41:16:43.80	8.25	
2	J004335+421219	00:43:35.23	+42:12:19.90	3.64	
3	J004337+412019	00:43:37.28	+41:20:19.40	8.92	
4	J004341+405435	00:43:41.76	+40:54:35.90	9.40	
5	J004345+412839	00:43:45.22	+41:28:39.90	4.91	

Table 14. Sample list of sources at 20 cm found in Project AC0308-c.

1 #	2 Name	3 RA (J2000)	4 DEC (J2000)	5 Flux (mJy)	6 Notes
1	J003651+404452	00:36:51.36	+40:44:52.40	4.81	
2	J003724+403821	00:37:24.96	+40:38:21.30	2.61	
3	J003730+401239	00:37:30.21	+40:12:39.10	4.95	
4	J003745+402513	00:37:45.61	+40:25:13.50	22.56	
5	J003807+405252	00:38:07.88	+40:52:52.90	3.04	

Table 15. Sample list of sources at 20 cm found in Project AC0496-a.

1 #	2 Name	3 RA (J2000)	4 DEC (J2000)	5 Flux (mJy)	6 Notes
1	J004057+415438	00:40:57.96	+41:54:38.20	1.17	
2	J004105+414451	00:41:05.89	+41:44:51.43	1.28	
3	J004112+415643	00:41:12.36	+41:56:43.10	1.63	
4	J004114+414339	00:41:14.21	+41:43:39.31	1.18	
5	J004129+413536	00:41:29.23	+41:35:36.41	1.02	

Table 16. Sample list of sources at 20 cm found in Project AH0139-a. Column 6 describes the source in additional projects.

1 #	2 Name	3 RA (J2000)	4 DEC (J2000)	5 Flux (mJy)	6 Notes
1	J004141+410343	00:41:41.34	+41:03:43.0	33.45	
2	J004147+411847	00:41:47.93	+41:18:48.0	30.44	Table:17 #20, Table:6 #11, Table:20 #11, Table:11 #7, Table:9 #8, Table:10 #11
3	J004151+411439	00:41:51.14	+41:14:39.4	17.68	Table:6 #12, Table:9 #9, Table:10 #12
4	J004218+412922	00:42:18.63	+41:29:22.6	245.11	
5	J004222+410805	00:42:22.03	+41:08:05.4	2.50	Table:9 #18, Table:10 #20

Table 17. Sample list of sources at 20 cm found in Project AH0221-a.

1 #	2 Name	3 RA (J2000)	4 DEC (J2000)	5 Flux (mJy)	6 Notes
1	J003933+404405	00:39:33.35	+40:44:05.34	4.16	
2	J003949+410421	00:39:49.41	+41:04:21.22	6.32	
3	J004012+410840	00:40:12.28	+41:08:40.73	2.85	
4	J004013+410839	00:40:13.28	+41:08:39.05	5.16	
5	J004013+410836	00:40:13.69	+41:08:36.59	6.31	

Table 18. Sample list of sources at 20 cm found in Project AH0524-a. Column 6 describes the source in additional projects.

1 #	2 Name	3 RA (J2000)	4 DEC (J2000)	5 Flux (mJy)	6 Notes
1	J003918+410301	00:39:18.49	+41:03:01.0	9.27	Table:19 #3
2	J003922+411040	00:39:22.15	+41:10:40.9	3.70	
3	J003931+411511	00:39:31.41	+41:15:11.8	2.36	
4	J003932+410440	00:39:32.22	+41:04:40.7	1.17	
5	J003935+411432	00:39:35.96	+41:14:32.7	4.74	Table:14 #37

Table 19. Sample list of sources at 20 cm found in Project AM0464-a.

1 #	2 Name	3 RA (J2000)	4 DEC (J2000)	5 Flux (mJy)	6 Notes
1	J003908+403009	00:39:08.78	+40:30:09.99	1.84	
2	J003916+403629	00:39:16.37	+40:36:29.37	0.59	
3	J003918+410300	00:39:18.55	+41:03:00.50	5.41	
4	J003919+402206	00:39:19.50	+40:22:06.08	0.74	
5	J003922+411038	00:39:22.16	+41:10:38.50	3.01	

Table 20. Sample list of sources at 20 cm found in Project AT0149-a.

1 #	2 Name	3 RA (J2000)	4 DEC (J2000)	5 Flux (mJy)	6 Notes
1	J004036+412404	00:40:36.79	+41:24:04.70	3.23	
2	J004037+412051	00:40:37.42	+41:20:51.49	3.78	
3	J004046+411637	00:40:46.52	+41:16:37.03	2.26	
4	J004049+411226	00:40:49.05	+41:12:26.92	2.30	
5	J004054+412632	00:40:54.52	+41:26:32.00	3.88	

Table 21. Flux density comparison (sample) between sources in common to $\lambda=20$ cm and $\lambda=92$ cm surveys of the M31. Columns 1, 2, 3 and 4 describes source information from the highest 20-cm resolution project available. Columns 5 and 6 from sources common across projects and integrated flux density (Col. 5) represent an average flux density across the are derived various project detections. Columns 7, 8, 9 and 10 are from Gelfand et al. (2004). Column 11 is the spectral index of Col. 5 and 9.

#	Source Name	Project #	RA (J2000)	DEC (J2000)	$S_{20\text{-cm}}$ (mJy)	$\Delta S_{20\text{-cm}}$ (mJy)	RA (J2000)	DEC (J2000)	$S_{92\text{-cm}}$ (mJy)	$\Delta S_{92\text{-cm}}$ (mJy)	α
1	J003807+405252	AC0308-c	00:38:07.88	+40:52:52.90	3.04	0.06	00:38:7.90	+40:52:53.75	7.03	0.67	-0.54933
2	J003904+410822	AB0437-a	00:39:04.30	+41:08:22.20	2.46	0.06	00:39:4.34	+41:08:18.21	8.54	0.69	-0.81555
3	J003918+411636	AC0308-c	00:39:18.45	+41:16:36.30	4.08	0.06	00:39:18.23	+41:16:36.85	23.39	1.29	-1.14424
4	J003927+405425	AB0437-b	00:39:27.05	+40:54:25.00	4.49	0.12	00:39:27.03	+40:54:26.57	10.48	0.74	-0.55542
5	J003933+404401	AM0464-a	00:39:33.02	+40:44:01.40	9.84	2.73	00:39:32.79	+40:43:59.63	18.14	2.85	-0.40081
6	J003932+400837	AC0308-c	00:39:32.83	+40:08:37.90	50.17	0.06	00:39:32.82	+40:08:36.74	126.12	8.99	-0.60404
7	J003948+403433	AM0464-a	00:39:48.29	+40:34:33.91	7.99	2.20	00:39:48.25	+40:34:35.00	16.20	5.27	-0.46316
8	J003949+410421	AH0221-a	00:39:49.41	+41:04:21.22	7.80	2.71	00:39:49.41	+41:04:20.91	15.68	0.99	-0.45797
9	J003950+402657	AM0464-a	00:39:50.41	+40:26:57.10	1.80	0.06	00:39:50.24	+40:26:55.81	6.82	0.76	-0.87287
10	J003956+411134	AB0437-b	00:39:56.37	+41:11:34.90	63.62	0.06	00:39:56.14	+41:11:37.89	106.35	7.11	-0.33668
11	J003957+411358	AH0524-a	00:39:57.59	+41:13:58.00	2.33	0.20	00:39:57.38	+41:13:58.60	6.46	0.57	-0.66822
12	J004005+401605	AC0308-c	00:40:05.32	+40:16:05.10	3.21	0.06	00:40:5.09	+40:16:8.15	5.40	0.64	-0.34082
13	J004006+402148	AM0464-a	00:40:06.40	+40:21:48.40	8.49	1.12	00:40:6.32	+40:21:45.83	21.63	1.29	-0.61319
14	J004013+410839	AH0221-a	00:40:13.28	+41:08:39.05	35.05	29.89	00:40:13.29	+41:08:42.35	68.40	4.71	-0.43811
15	J004016+405824	AH0221-a	00:40:16.93	+40:58:24.36	21.58	7.55	00:40:16.79	+40:58:25.32	61.06	4.45	-0.68159
16	J004017+395508	AC0308-c	00:40:17.24	+39:55:08.10	15.54	0.06	00:40:17.13	+39:55:4.17	190.41	9.23	-1.64195
17	J004024+412926	AC0308-c	00:40:24.13	+41:29:26.70	6.09	0.06	00:40:24.11	+41:29:27.98	24.36	1.41	-0.90840
18	J004024+410712	AH0221-a	00:40:24.36	+41:07:12.95	26.96	11.04	00:40:24.51	+41:07:12.58	83.05	5.94	-0.73731
19	J004024+412029	AH0524-a	00:40:24.84	+41:20:29.50	8.82	0.55	00:40:24.65	+41:20:32.44	9.73	0.72	-0.06434
20	J004030+402755	AM0464-a	00:40:30.30	+40:27:55.50	6.18	1.55	00:40:30.29	+40:27:54.50	10.15	0.79	-0.32476
21	J004035+413511	AC0308-c	00:40:35.58	+41:35:11.10	16.02	0.06	00:40:35.75	+41:35:10.89	12.81	0.82	0.14653
22	J004044+404846	AH0221-a	00:40:44.29	+40:48:46.59	12.66	4.15	00:40:44.35	+40:48:45.42	34.27	3.65	-0.65274
23	J004047+405525	AH0221-a	00:40:47.11	+40:55:25.17	2.60	0.43	00:40:47.05	+40:55:24.20	3.69	0.42	-0.22942
24	J004055+405723	AH0221-a	00:40:55.88	+40:57:23.48	28.16	2.61	00:40:55.90	+40:57:23.34	153.25	7.59	-1.11024
25	J004057+415438	AC0496-a	00:40:57.96	+41:54:38.20	1.17	0.06	00:40:58.08	+41:54:37.59	23.45	2.62	-1.96442
26	J004100+411354	AH0524-a	00:41:00.26	+41:13:54.40	5.74	2.83	00:41:0.18	+41:13:54.90	12.79	0.86	-0.52558
27	J004103+410430	AH0524-a	00:41:03.03	+41:04:30.30	2.68	0.21	00:41:2.91	+41:04:27.99	3.36	0.41	-0.14940
28	J004111+402411	AH0221-a	00:41:11.30	+40:24:11.01	11.55	1.02	00:41:11.33	+40:24:10.59	51.26	2.58	-0.97631
29	J004111+403328	AM0464-a	00:41:11.43	+40:33:28.70	5.37	0.49	00:41:11.74	+40:33:28.97	15.67	0.96	-0.70174
30	J004112+412454	AH0524-a	00:41:12.82	+41:24:54.38	9.01	0.06	00:41:12.88	+41:24:57.51	28.65	2.89	-0.75803

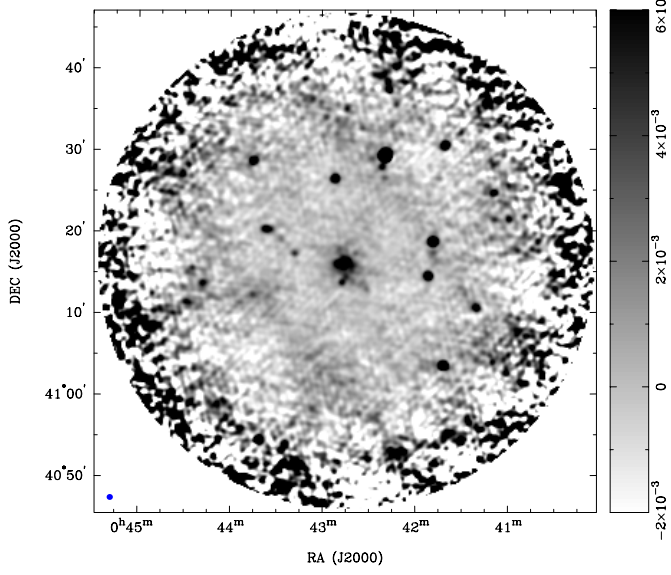


Fig. 1. VLA Project AC0101 radio-continuum total intensity image of M31. The synthesised beam, as represented by the blue circle in the lower left hand corner, is $45.9'' \times 43.2''$ and the r.m.s noise is 0.49 mJy/beam.

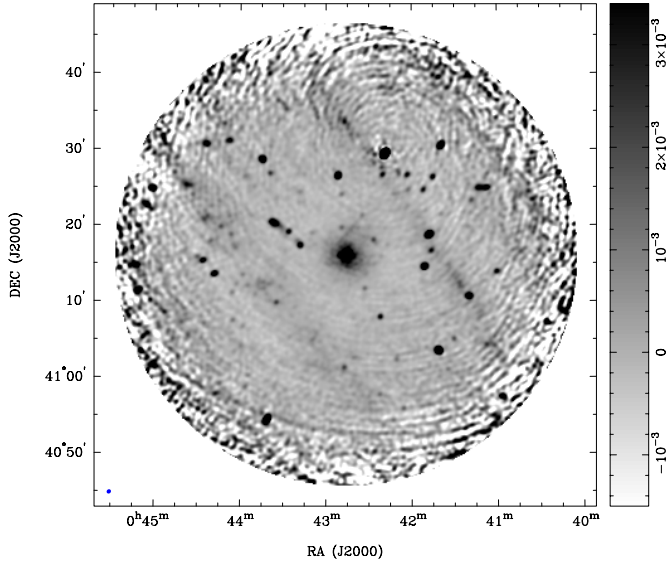


Fig. 2. VLA Project AB0551 radio-continuum total intensity image of M31. The synthesised beam, as represented by the blue circle in the lower left hand corner, is $35.9'' \times 32.1''$ and the r.m.s noise is 0.12 mJy/beam. This image is in terms of Jy/Beam.

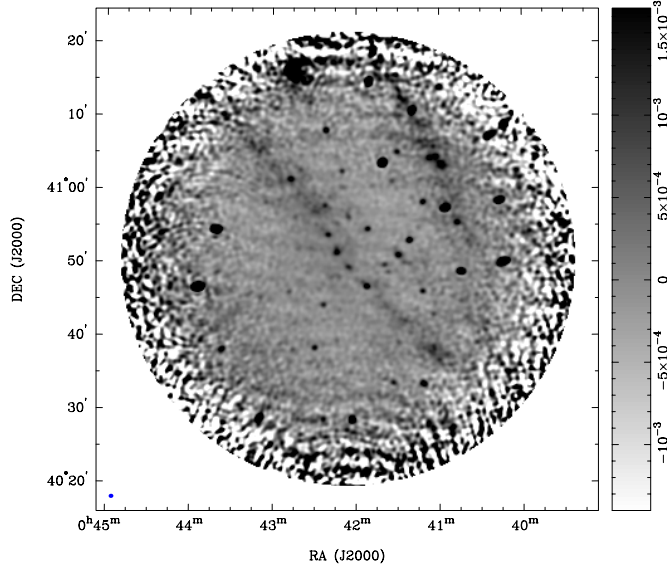


Fig. 3. VLA Project AB0491 radio-continuum total intensity image of M31. The synthesised beam, as represented by the blue circle in the lower left hand corner, is $39.0'' \times 33.8''$ and the r.m.s noise is 0.12 mJy/beam. This image is in terms of Jy/Beam.

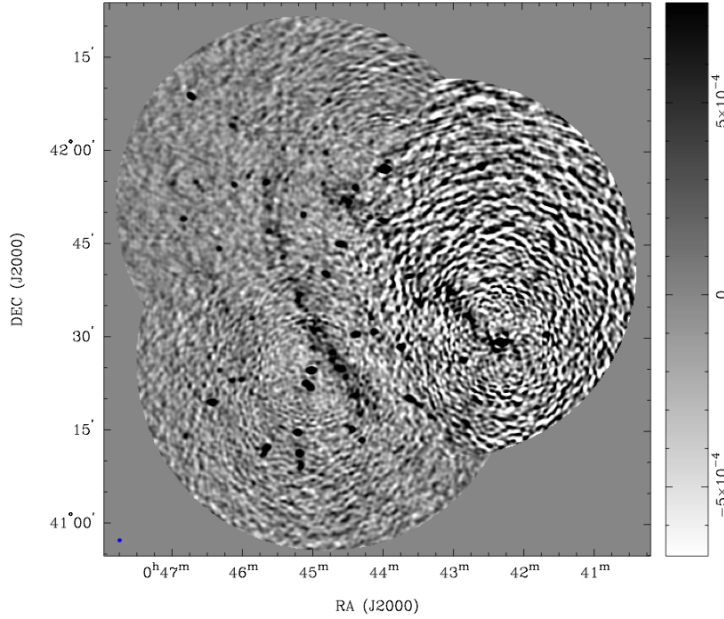


Fig. 4. VLA Project AB0647, segment a, radio-continuum total intensity image of M31. The synthesised beam, as represented by the blue circle in the lower left hand corner, is $41.2'' \times 37.3''$ and the r.m.s noise is 0.24 mJy/beam. This image is in terms of Jy/Beam.

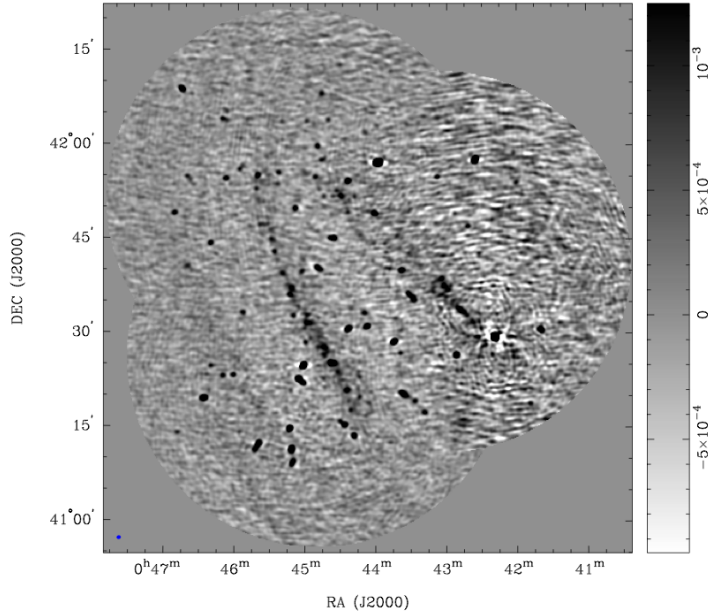


Fig. 5. VLA Project AB0647, segment *b*, radio-continuum total intensity image of M31. The synthesised beam, as represented by the blue circle in the lower left hand corner, is $40.9'' \times 35.4''$ and the r.m.s noise is 0.24 mJy/beam. This image is in terms of Jy/Beam.

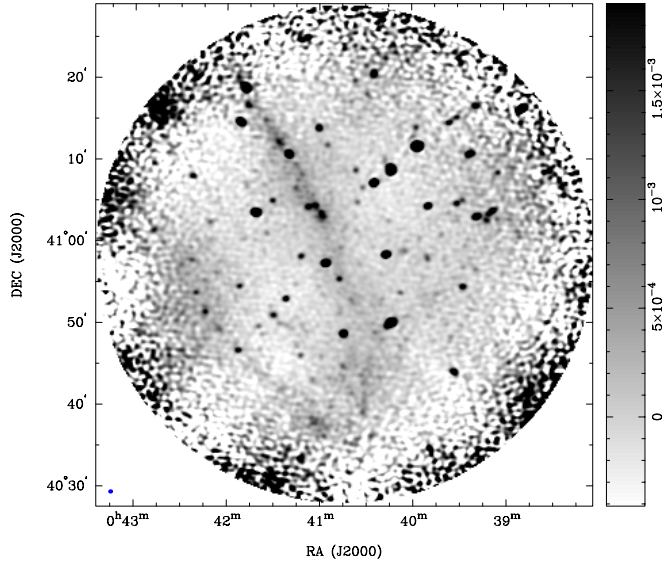


Fig. 6. VLA Project AB0437, segment *a*, radio-continuum total intensity image of M31. The synthesised beam, as represented by the blue circle in the lower left hand corner, is $36.0'' \times 31.0''$ and the r.m.s noise is 0.10 mJy/beam. This image is in terms of Jy/Beam.

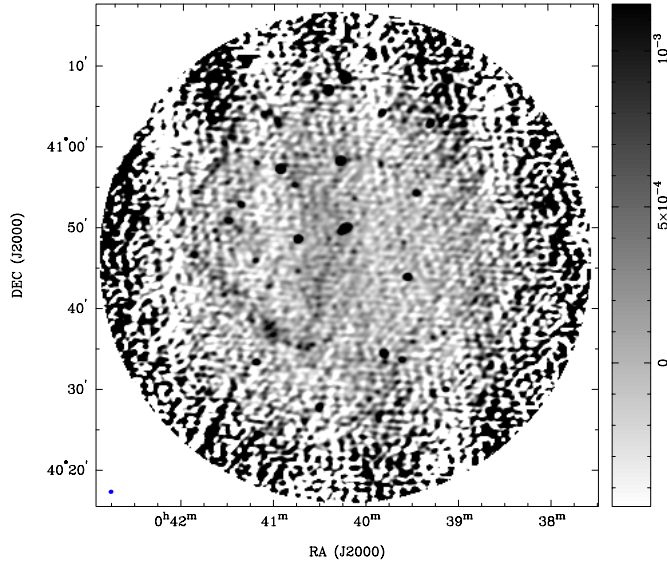


Fig. 7. VLA Project AB0437, segment *b*, radio-continuum total intensity image of M 31. The synthesised beam, as represented by the blue circle in the lower left hand corner, is $36.0'' \times 31.1''$ and the r.m.s noise is 0.19 mJy/beam. This image is in terms of Jy/Beam.

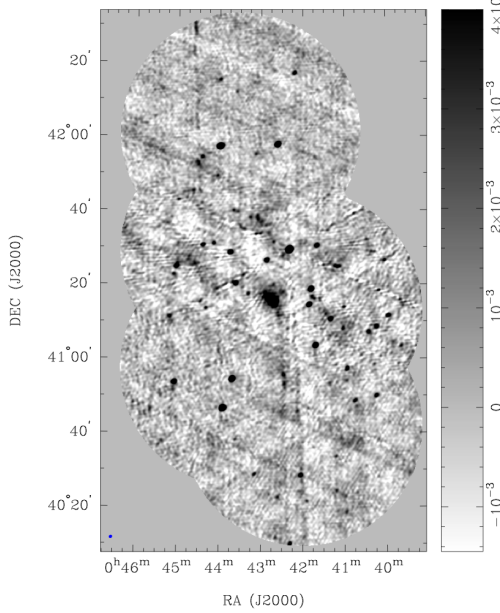


Fig. 8. VLA Project AC0308, segment *a*, radio-continuum total intensity image of M 31. The synthesised beam, as represented by the blue circle in the lower left hand corner, is $57.9'' \times 49.8''$ and the r.m.s noise is 0.72 mJy/beam. This image is in terms of Jy/Beam.

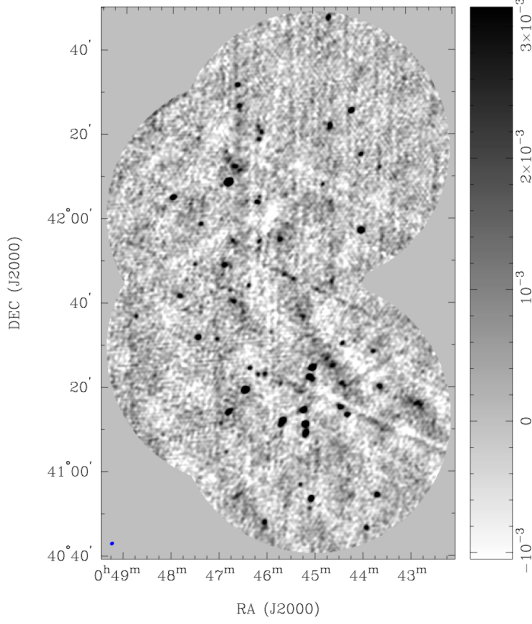


Fig. 9. VLA Project AC0308, segment *b*, radio-continuum total intensity image of M31. The synthesised beam, as represented by the blue circle in the lower left hand corner, is $58.9'' \times 48.9''$ and the r.m.s noise is 0.54 mJy/beam. This image is in terms of Jy/Beam.

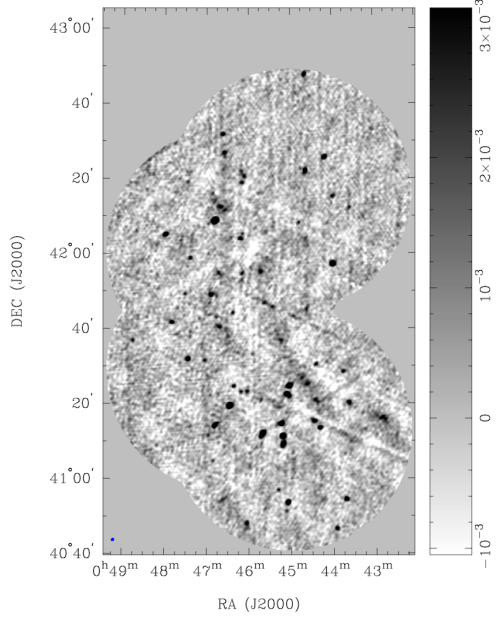


Fig. 10. VLA Project AC0308, segment *c*, radio-continuum total intensity image of M31. The synthesised beam, as represented by the blue circle in the lower left hand corner, is $58.0'' \times 50.2''$ and the r.m.s noise is 0.60 mJy/beam. This image is in terms of Jy/Beam.

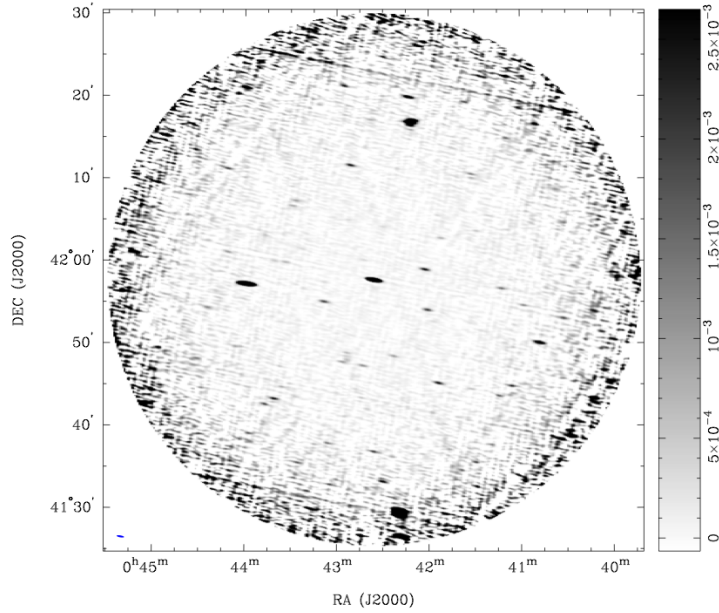


Fig. 11. VLA Project AC0496 radio-continuum total intensity image of M31. The synthesised beam, as represented by the blue circle in the lower left hand corner, is $54.6'' \times 14.0''$ and the r.m.s noise is 0.08 mJy/beam. This image is in terms of Jy/Beam.

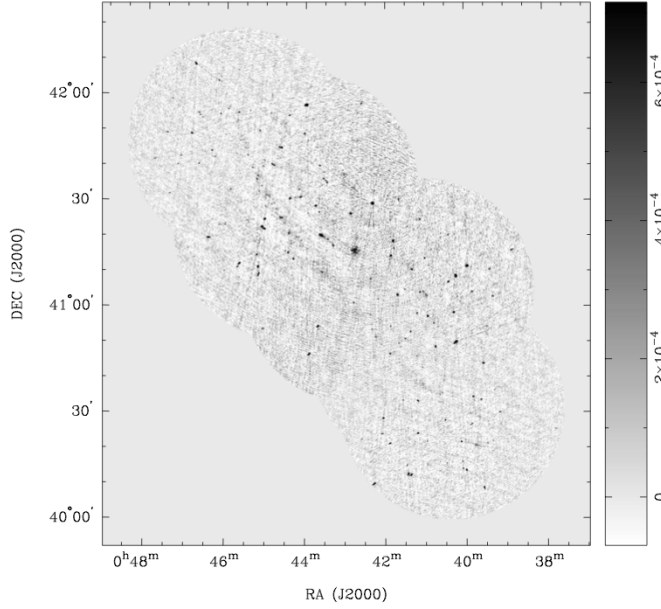


Fig. 12. VLA Project AM0464 radio-continuum total intensity image of M31. The synthesised beam is $12.8'' \times 12.2''$ and the r.m.s noise is 0.13 mJy/beam. This image is in terms of Jy/Beam.

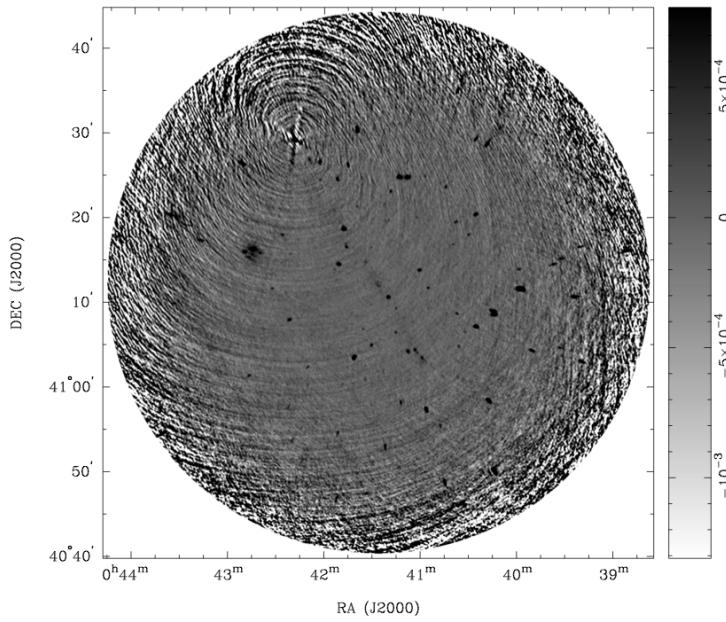


Fig. 13. VLA Project AH0524 radio-continuum total intensity image of M31. The synthesised beam is $12.8'' \times 12.2''$ and the r.m.s noise is 0.07 mJy/beam. This image is in terms of Jy/Beam.

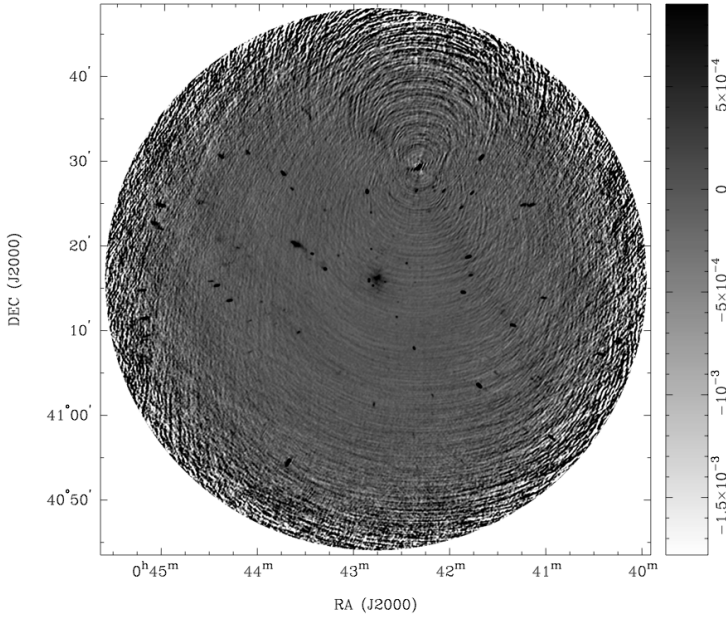


Fig. 14. VLA Project AB0679, segment a, radio-continuum total intensity image of M31. The synthesised beam is $12.0'' \times 11.7''$ and the r.m.s noise is 0.07 mJy/beam. This image is in terms of Jy/Beam.

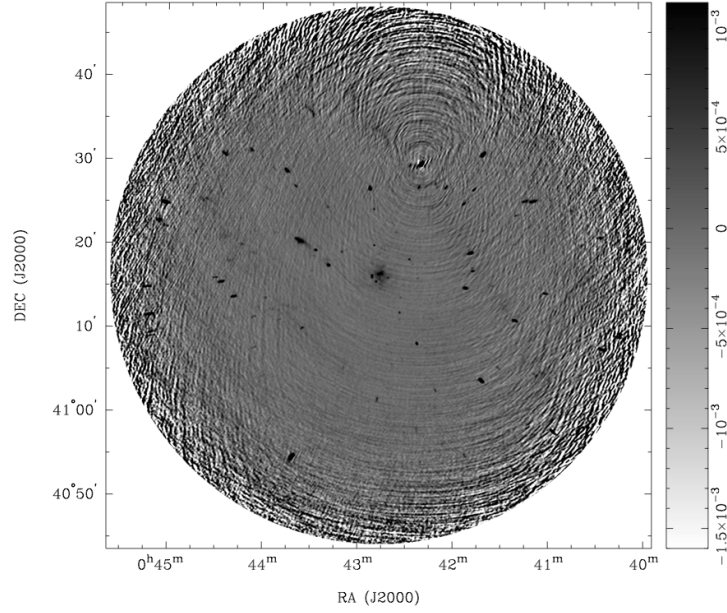


Fig. 15. VLA Project AB0679, segment b, radio-continuum total intensity image of M31. The synthesised beam is $12.1'' \times 11.5''$ and the r.m.s noise is 0.08 mJy/beam. This image is in terms of Jy/Beam.

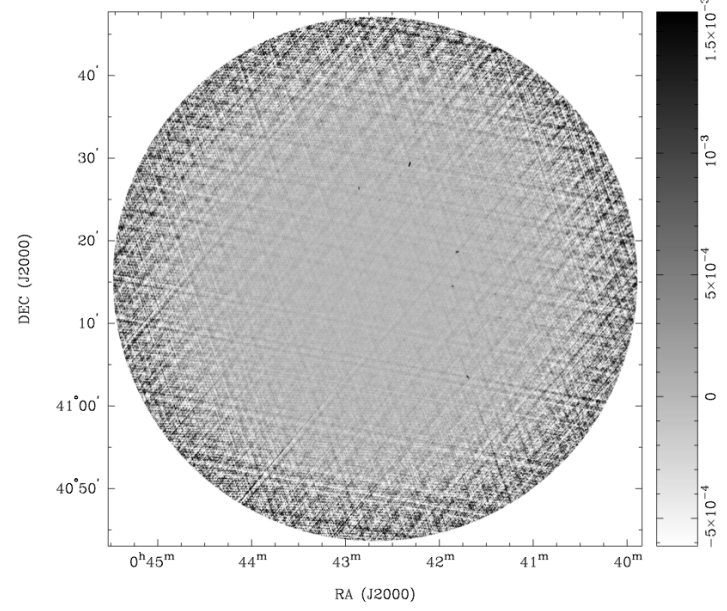


Fig. 16. VLA Project AT0149 radio-continuum total intensity image of M31. The synthesised beam is $4.0'' \times 3.4''$ and the r.m.s noise is 0.08 mJy/beam. This image is in terms of Jy/Beam.

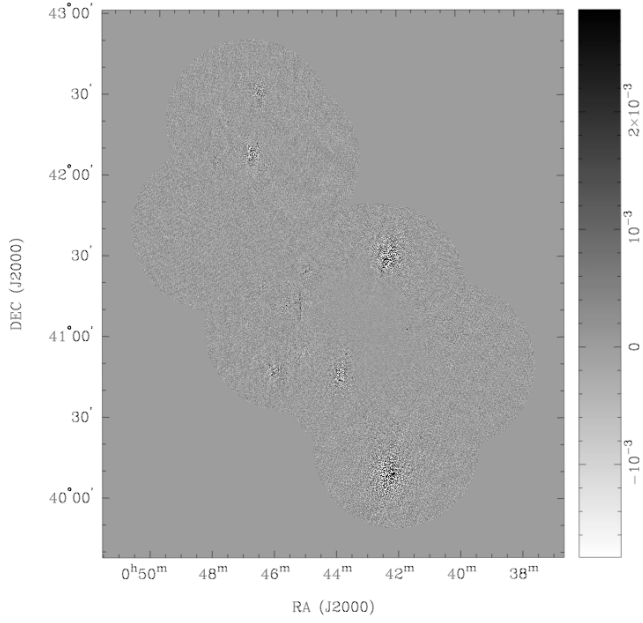


Fig. 17. VLA Project AH0221 radio-continuum total intensity image of M31. The synthesised beam is $3.4'' \times 3.2''$ and the r.m.s noise is 0.22 mJy/beam. This image is in terms of Jy/Beam.

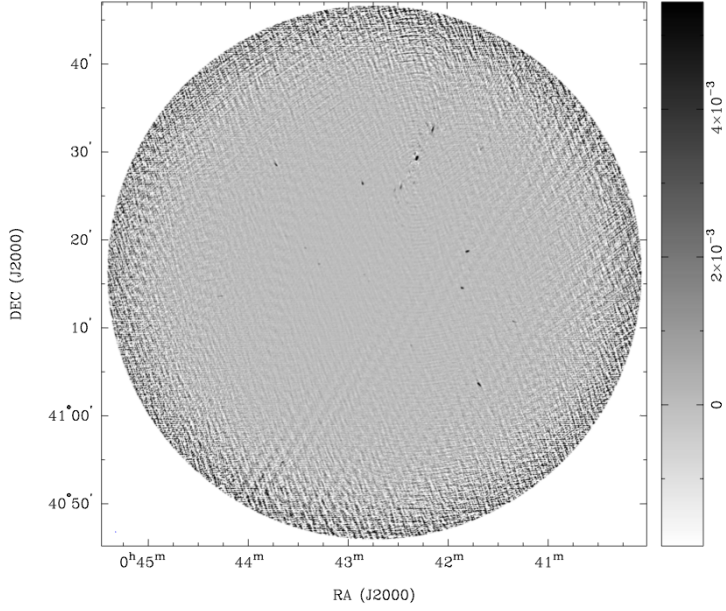


Fig. 18. VLA Project AH0139 radio-continuum total intensity image of M31. The synthesised beam is $7.2'' \times 6.6''$ and the r.m.s noise is 0.16 mJy/beam. This image is in terms of Jy/Beam.

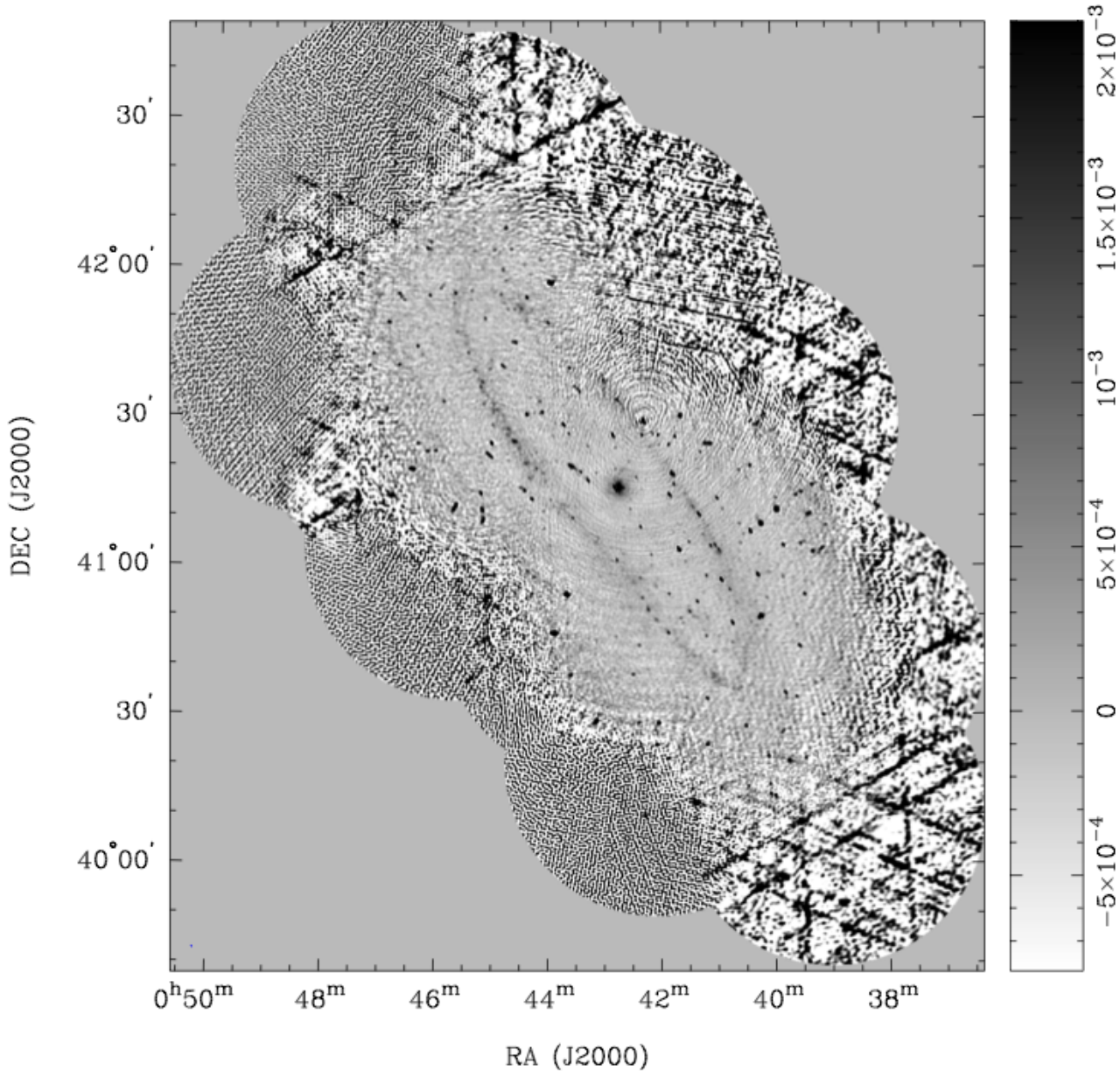


Fig. 19. A mosaiced radio-continuum total intensity image of M31 produced with all fully polarised VLA observations with a uv restriction of $0\text{--}5\text{ k}\lambda$. The synthesised beam, as represented by the blue circle in the lower left hand corner, is $35.73'' \times 16.38''$ and the r.m.s noise is 0.145 mJy/beam . This image is in Jy/Beam.

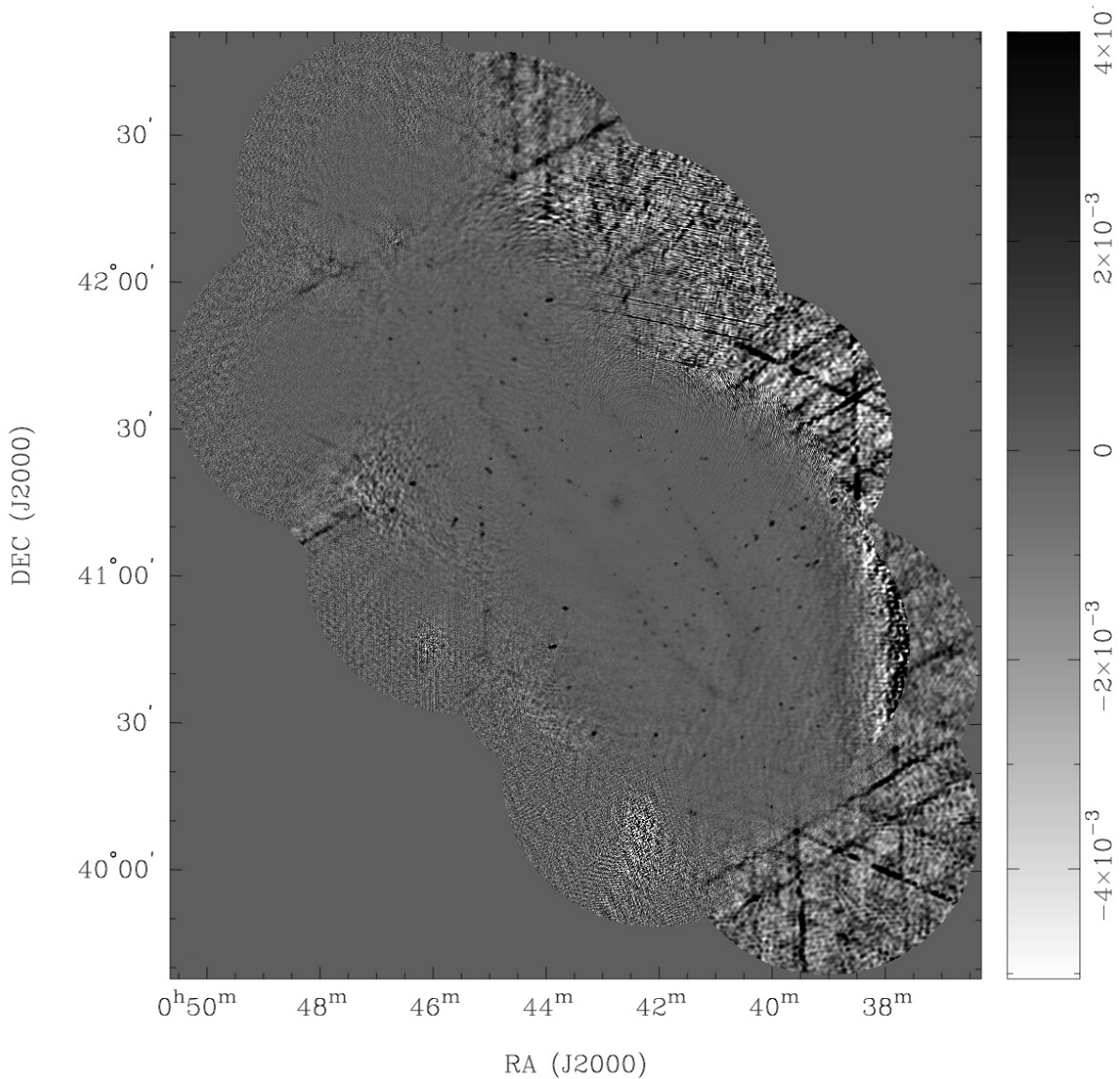


Fig. 20. A mosaiced radio-continuum total intensity image of M31 produced with all fully polarised VLA observations. The synthesised beam is $6.14'' \times 5.35''$ and the r.m.s noise is 0.09 mJy/beam. This image is in Jy/Beam.

DEC (J2000)

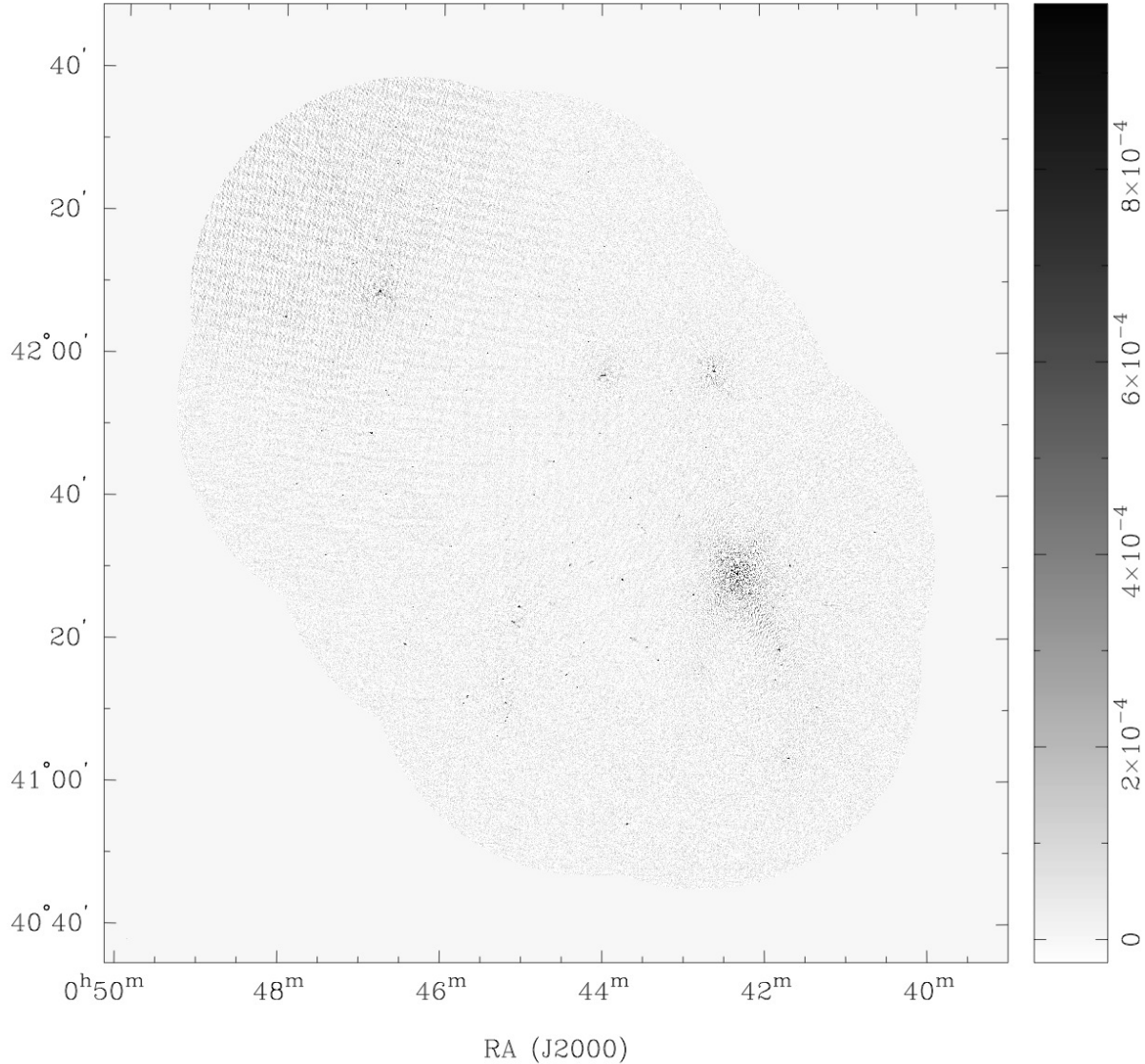


Fig. 21. A mosaiced radio-continuum total intensity image of M31 produced with VLA project AB0396 and AB0999. The synthesised beam is $4.63'' \times 3.78''$ and the r.m.s noise is 0.08 mJy/beam. This image is in terms of Jy/Beam.

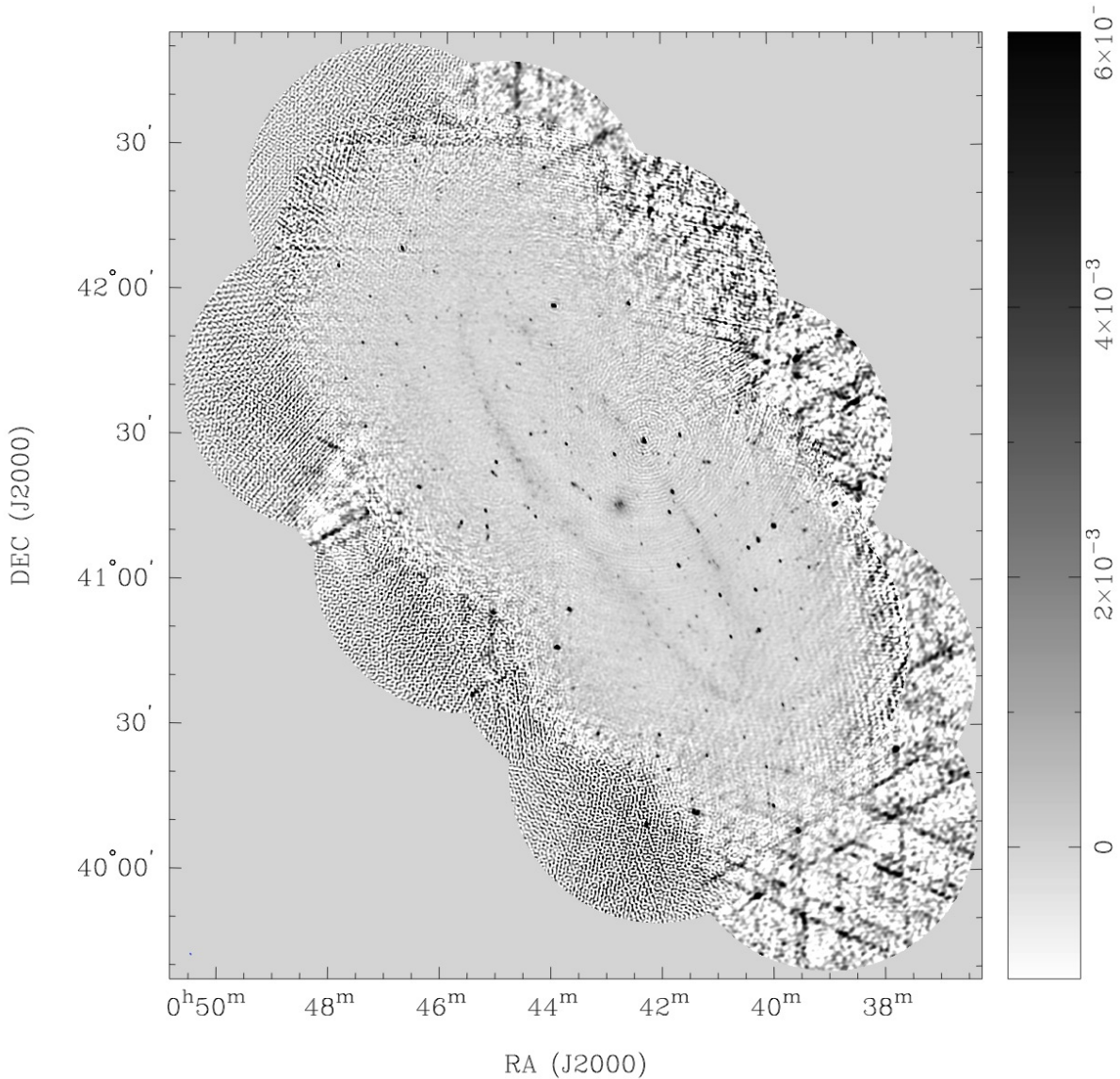


Fig. 22. A mosaiced radio-continuum total intensity image of M31 produced with all calibrated VLA observations. The synthesised beam, as represented by the blue circle in the lower left hand corner, is $32.61'' \times 16.36''$ and the r.m.s noise is 0.13 mJy/beam. This image is in terms of Jy/Beam.

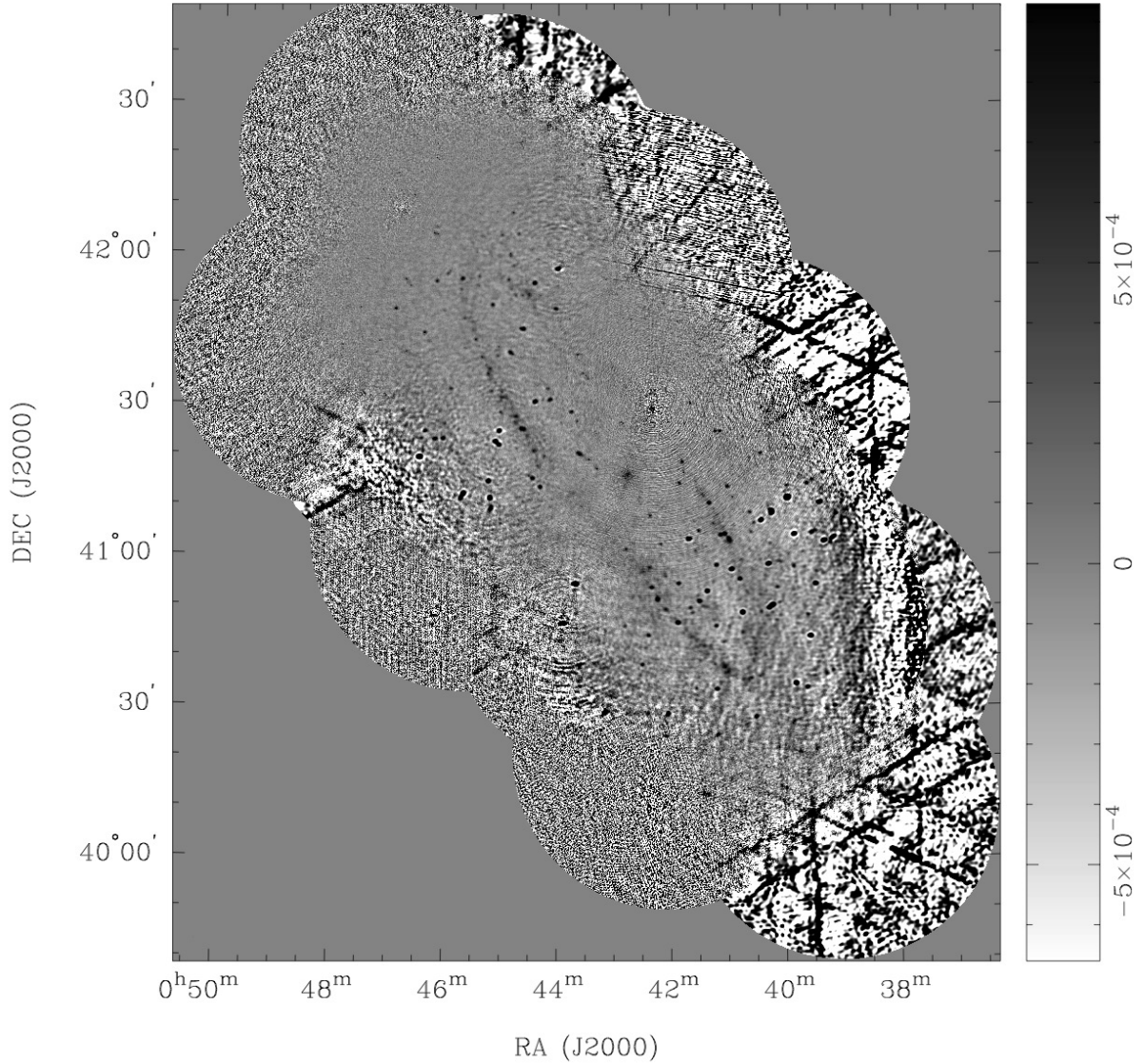


Fig. 23. A mosaiced radio-continuum total intensity image of M31 produced with all calibrated VLA observations. The synthesised beam is $6.13'' \times 5.35''$ and the r.m.s noise is 0.12 mJy/beam. This image is in terms of Jy/Beam.

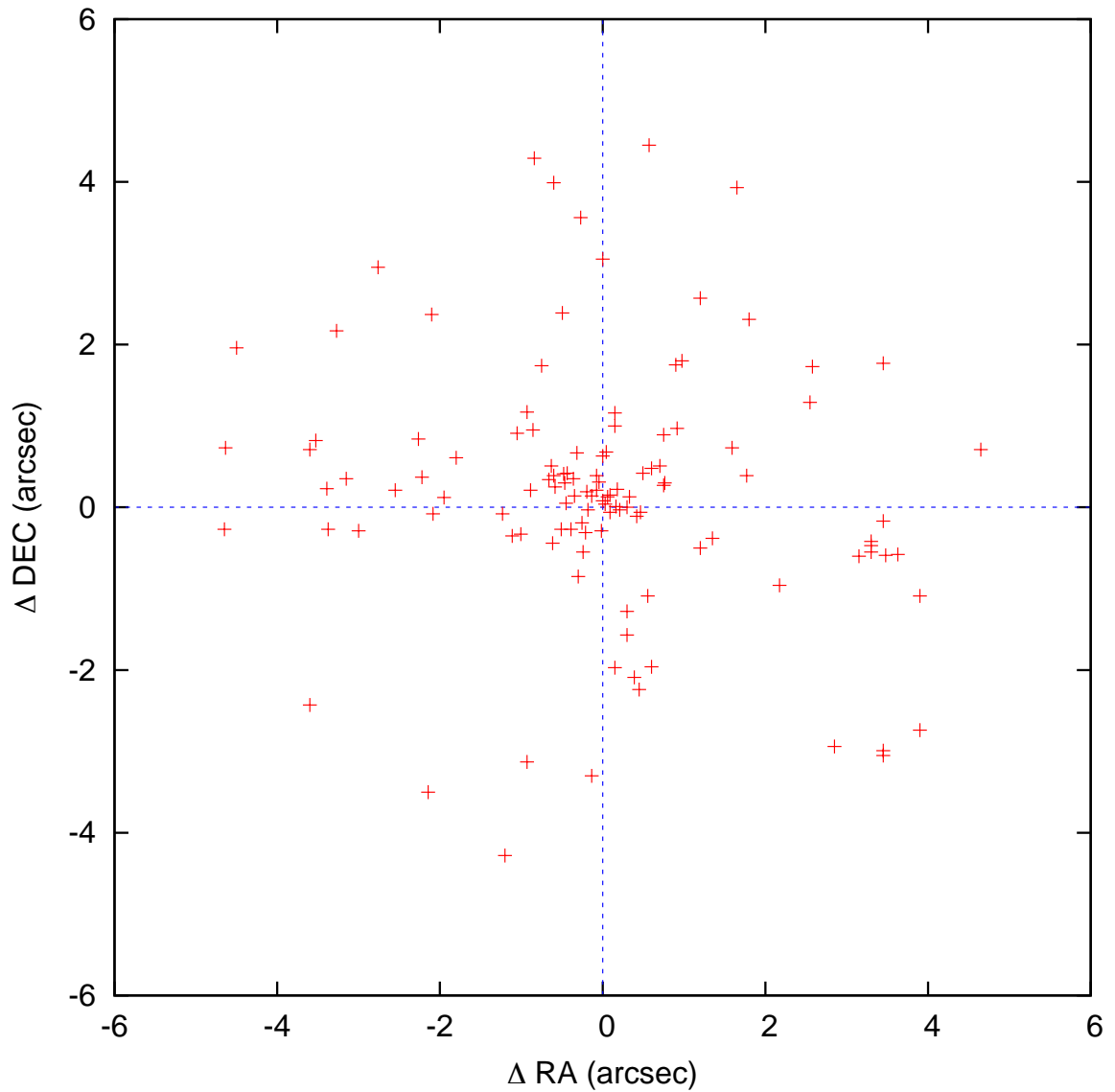


Fig. 24. Comparison of positional differences (ΔRA and ΔDEC) between our catalogue and Gelfand et al. (2004).

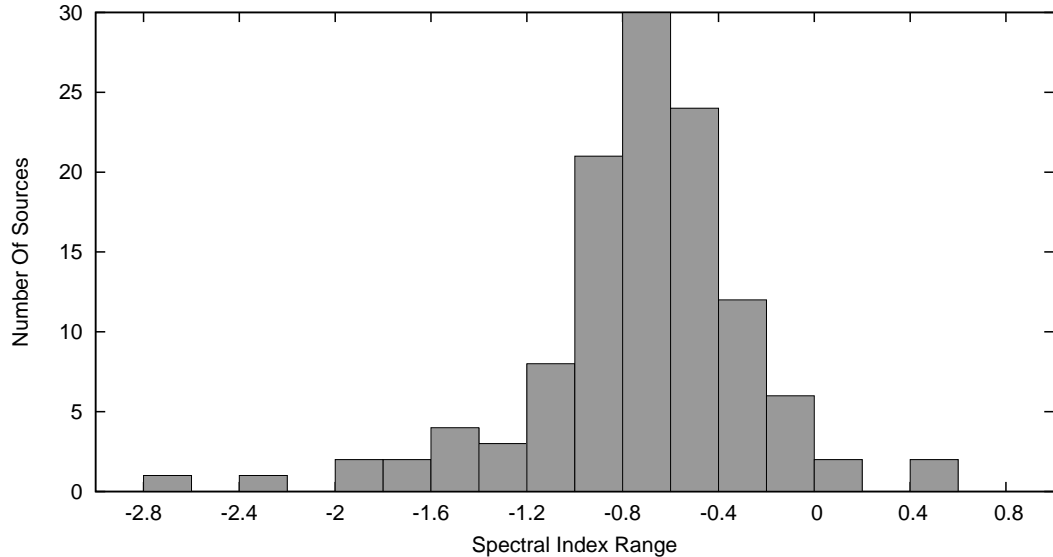


Fig. 25. Spectral index distribution of point sources in the field of M 31.

6. Conclusions

We present new $\lambda=20$ cm ($\nu=1.4$ GHz) images of M 31 constructed from archived VLA radio-continuum observations. These new images consisting of 17 individual VLA projects which are of high-sensitivity and resolution. Images presented here are sensitive to $\text{rms}=60\ \mu\text{Jy}$ and feature a high angular resolution ($<10''$). Also, we present a complete sample of 864 unique discrete radio sources across the field of M 31. The most prominent region in M 31 is “the ring feature” for which we estimate a total integrated flux density of 706 mJy at $\lambda=20$ cm. From our 20-cm catalogue, we find 118 discrete sources that are in common to those listed in Gelfand et al. (2004) at $\lambda=92$ cm. The majority (61%) of these sources exhibit a spectral index of $\alpha < -0.6$ indicating predominant non-thermal emission which is more typical of background objects.

Acknowledgements – We used the KARMA and MIRIAD software packages developed by the ATNF. The National Radio Astronomy Observatory is a facility of the National Science Foundation operated under cooperative agreement by Associated Universities, Inc.

REFERENCES

- Braun, R.: 1990a, *Aust. J. Phys. Astrophys. Suppl.*, **72**, 755.
- Braun, R.: 1990b, *Aust. J. Phys. Astrophys. Suppl.*, **72**, 761.
- Dickel, J. R., Dodorico, S.: 1984, *Mon. Not. R. Astron. Soc.*, **206**, 351.
- Dickel, J. R., Dodorico, S., Felli, M., Dopita, M.: 1982, *Aust. J. of Phys.*, **252**, 582.
- Galvin, T. J.: et al., 2012, *Astrophys. Space Sci.*, in press.
- Gelfand, J. D., Lazio, T. J. W., Gaensler, B. M., 2004, *Aust. J. Phys. Astrophys. Suppl.*, **155**, 89.
- Gooch, R.: 1996, in ”Astronomical Society of the Pacific Conference Series, Vol. 101, Astronomical Data Analysis Software and Systems V”, G. H. Jacoby & J. Barnes, ed., 80.
- Karachentsev, I. D., Karachentseva, V. E., Huchtmeier, W. K., Makarov, D. I.: 2004, *Astron. J.*, **127**, 2031.
- Payne, J. L., Filipović, M. D., Pannuti, T. G., Jones, P. A., Duric N., White, G. L., Carpano, S.: 2004, *Astron. Astrophys.*, **425**, 443.
- Sault, R. J., Teuben, P. J., Wright, M. C. H.: 1995, in ”Astronomical Society of the Pacific Conference Series, Vol. 77, Astronomical Data Analysis Software and Systems IV”, R. A. Shaw, H. E. Payne, & J. J. E. Hayes, ed., 433.
- Steer, D. G., Dewdney, P. E., Ito, M. R.: 1984, *Astron. Astrophys.*, **137**, 159.

**НОВО ПРОУЧАВАЊЕ М 31 У РАДИО-КОНТИНУМУ НА
20 ЦМ – МАПЕ И КАТАЛОЗИ ТАЧКАСТИХ ИЗВОРА**

T. J. Galvin, M. D. Filipović, E. J. Crawford, N. F. H. Tothill, G. F. Wong, A. Y. De Horta

University of Western Sydney, Locked Bag 1797, Penrith South DC, NSW 2751, AUSTRALIA
E-mail: *m.filipovic@uws.edu.au*

УДК ...
Оригинални научни рад

У овој студији представљамо нове Very Large Array (VLA) радио-континум мапе и каталоге тачкастих објеката у пољу М 31 на $\lambda=20$ см ($\nu=1.4$ GHz). Нове мапе високе резолуције ($<10''$) и осетљивости ($\text{rms}=60 \mu\text{Jy}$) су направљене спајањем свих 17 архивираних посматрања VLA телескопа. Комплетан каталог свих објеката у пољу М 31 галаксије садржи 864 радио извора. Ови објекти су

упоређени са Gelfand et al. (2004) каталогом на $\lambda=92$ см и нађено је 118 заједничких радио извора у оба каталога. Већина ових објеката (61%) имају веома стрм радио спектрални индекс ($\alpha <-0.6$) што је типично за нетермалне изворе који се налазе ван М 31 галаксије. Детектовали смо и један од најпроминентнијих области у М 31 галаксији – прстен – са укупном густином флуksа од 706 mJy на $\lambda=20$ см.